

Biometallic Synthesis of Gel-Loaded Copper Nanoparticles Using *Manilkara zapota* L. Extract: Phytochemical Profiling and Breast Cancer Evaluation

Ms Kiran Mali^{1*}, Dr Rita Chakole²

¹Research Scholar, Department of Pharmaceutics, Government College of Pharmacy, Karad- India- 415124.

²Associate Professor, Department of Pharmaceutical Chemistry, Government College of Pharmacy, Karad- India- 415124.

*Corresponding author: kiran.pharma1997@gmail.com

How to cite this article: Ms Kiran Mali, Dr Rita Chakole (2024) Biometallic Synthesis of Gel-Loaded Copper Nanoparticles Using *Manilkara zapota* L. Extract: Phytochemical Profiling and Breast Cancer Evaluation. *Library Progress International*, 44(6), 1248-1263

Abstract:

Background: *Manilkara zapota* L. is rich in bioactive phytochemicals with reported anticancer properties. The incorporation of copper nanoparticles (CuNPs) into Carbopol gels may increase their therapeutic potential and facilitate controlled, pH-sensitive delivery.

Methods: Petroleum ether extracts of *M. zapota* aerial part were prepared and phytochemically characterized via qualitative analysis, HPTLC, and GC-MS. CuNPs were synthesized via green reduction and incorporated into a Carbopol gel. The formulation was evaluated for its particle size, zeta potential, morphology, entrapment efficiency, stability, pH-sensitive release, and cytotoxic potential against MCF-7 breast cancer cells and MCF-10A normal cells.

Results: The extract contained phenols, flavonoids, anthocyanins, steroids, and cardiac glycosides. HPTLC bands were observed at R_f values of 0.70, 0.76, and 0.88. The major GC-MS compounds included β -sitosterol acetate, 3 β -acetoxystigmasta-4,6,22-pentatriacontene. The CuNPs were 286.2 nm in size with a zeta potential of -6.6 mV and 86.83% entrapment efficiency. The gel demonstrated optimal viscosity, pH 6.8–7.4, sustained release (pH 6.5: 91.53%, pH 7.4: 72.56%), cytotoxicity against MCF-7 cells (IC₅₀ = 36.04 μ g/mL), minimal toxicity to MCF-10A cells, and stability over 3 months. The release kinetics followed the Korsmeyer–Peppas model (n = 0.58).

Conclusion: The CuNP-loaded gel from *M. zapota* extract exhibited sustained, pH-sensitive, and selective anticancer activity with excellent stability, supporting its potential translational application.

Keywords: *Manilkara zapota*, Breast cancer, Phytochemicals, Herbal therapy, Copper nanoparticles, Cuproptosis, Green synthesis, Carbopol 940

1. Introduction:

Breast cancer continues to be one of the most frequently diagnosed malignancies and a leading cause of mortality among women worldwide. Recent estimates from the World Health Organization suggest that approximately 1.3 million new cases are reported annually, making it a persistent global health concern [1-3]. Although progress has been made in early screening and chemotherapy, the limitations of current treatments, such as systemic toxicity, drug resistance, and restricted therapeutic selectivity, remain major obstacles. These challenges highlight the need to explore safer and more effective

treatment strategies. Medicinal plants have long been valued as a source of therapeutic compounds. Compared with many synthetic drugs, phytochemicals, which are naturally occurring bioactive molecules within these plants, are generally regarded as safer and easier for the human body to metabolize [4-9]. Historically, plant-derived compounds have contributed significantly to modern medicine, with a considerable proportion of clinically available drugs originating from natural sources [10-13]. In oncology, phytochemicals not only demonstrate direct cytotoxicity but also provide structural templates for the development of novel anticancer agents.

Nanotechnology has introduced innovative strategies for improving drug delivery and cancer therapy [13-17]. In particular, copper has emerged as a promising anticancer agent because of its role in cuproptosis, a regulated form of cell death. This process involves copper interaction with mitochondrial lipoylated proteins, leading to metabolic disruption, proteotoxic stress, and eventual tumor cell death. Unlike conventional apoptosis, cuproptosis can bypass chemotherapy resistance and promote immunogenic cell death, thereby enhancing antitumor immune responses [18-22]. The green synthesis of copper nanoparticles using phytoconstituents offers an environmentally friendly and cost-effective route, with the added benefit of natural compounds acting as both reducing and stabilizing agents [23-29]. The incorporation of these nanoparticles into Carbopol-based gel further improves their therapeutic potential by enabling sustained release, favorable rheological properties, and enhanced local retention [30-34]. Carbopol, a synthetic but biocompatible polymer, is widely used in topical and transdermal formulations because of its stability, safety, and excellent gelling capacity, making it a suitable matrix for gel development in cancer therapy [35-40]. The present work aimed to synthesize copper nanoparticles (CuNPs) from *M. zapota* L. extract, integrate them into a Carbopol gel system, and evaluate their physicochemical features, release characteristics, and anticancer potential against breast cancer cells.

2. Materials and methods

2.1. Materials:

The aerial parts of *M. zapota* were collected from a rural region in Maharashtra, India (latitude: 17.1810° N; longitude: 74.1159° E), from February to April. The solvents used for extraction were petroleum ether, copper sulfate, Carbopol 940, and ethanol, which were procured from Loba Chemicals (India) and were of analytical grade.

2.2. Methods:

2.2.1. Plant collection and authentication:

The collected plant material was taxonomically authenticated by a certified taxonomist and assigned a voucher number (BSI/WRC/Iden.Cer. / 2022/0810220017786: MKKWT-2), which was deposited at the Botanical Survey of India [41]. Figure 1 shows the authenticated specimen and the morphological features of *M. zapota*. The aerial parts, collected during the flowering and fruiting seasons, were shade-dried for 4–5 days and then pulverized as shown in Figure 2 to a medium-coarse powder to increase extraction efficiency. [42-43].

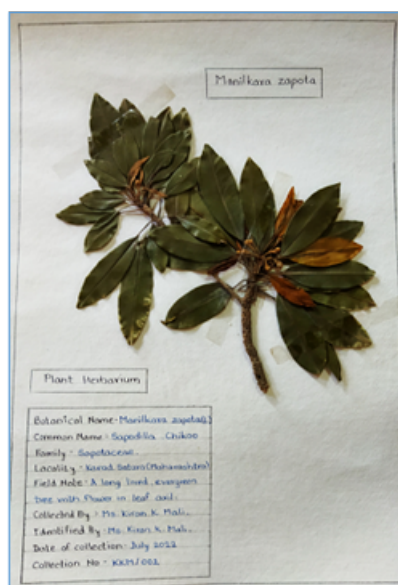


Figure 1. Herbarium of *Manilkara zapota* (family Sapotaceae)



Figure 2. Reduction in the size of plant material and the storage of powder in an airtight container

2.2.2. Extraction:

Successive Soxhlet extraction was performed as shown in Figure 3 using petroleum ether. The extraction temperature was maintained at the solvent's boiling point during the Soxhlet procedure. All the obtained extracts were completely dried and stored in airtight containers. The percentage yield for each extract was calculated via the following formula [44-47]:

$$\text{Extraction yield (\%)} = \left(\frac{\text{weight of extract obtained}}{\text{weight of dry plant material used}} \right) * 100$$



Figure 3. Soxhlet extraction

2.2.3. Phytochemical evaluation of extract:

Qualitative phytochemical screening of *M. zapota* extracts was conducted to identify the major classes of secondary metabolites via standard procedures. Reddish-brown precipitates identified alkaloids with Wagner's reagent, whereas phenols were indicated by a bluish-black coloration upon reaction with ferric chloride. Flavonoids produced yellow coloration under alkaline conditions that disappeared after acidification, whereas anthocyanins exhibited a characteristic shift from pink-red to blue-violet with changes in pH. Tannins were confirmed by the formation of a white precipitate with gelatin, mucilage with a cloudy mass after alcohol addition, and saponins were confirmed by persistent freezing upon shaking with water. Steroids and triterpenes are distinguished by distinct color reactions with concentrated sulfuric acid, resins by an orange-to-yellow transition with acetic anhydride, and cardiac glycosides by the appearance of bluish-green and reddish-brown layers. These reactions collectively confirmed the presence of a broad spectrum of phytochemicals in the extracts [48-50].

2.2.4. HPTLC:

Approximately 50 mg of the powdered extract was dissolved in 5 mL of methanol, vortexed for 5–10 minutes, sonicated for 15 minutes, and centrifuged at 3000 rpm for 15 minutes. The resulting supernatant was filtered and stored in vials. The samples were diluted in a 1:1 ratio with methanol if overly concentrated [51].

Chromatographic Conditions:

Stationary phase: TLC plates coated with silica gel 60 F₂₅₄ (Merck, Product No. 1.05554.0007)

Development distance: 70 mm

Mobile phase: Toluene: ethyl acetate: formic acid (5:4:1 v/v/v)

Saturation time: 20 minutes

2.2.5. Environmentally Benign Synthesis of Copper Nanoparticles (CuNPs) via the Petroleum Ether Extract of *M. zapota*:

CuNPs were synthesized by dissolving 0.49 g of CuSO₄·5H₂O in 20 mL of deionized water with

magnetic stirring (30 min). The petroleum ether extract of *M. zapota* (20 mL) was added dropwise, and the mixture was stirred for 3 h at room temperature until the color shifted from pale green to brown. The pH was adjusted with aqueous ammonia to promote reduction and precipitation. The nanoparticles were recovered, washed sequentially with deionized water and ethanol, dried at 60 °C, and stored in airtight containers for further characterization and biological assays [52].

2.2.6. Formation of Carbopol gel:

Copper nanoparticles (CuNPs) were incorporated into a 1% w/v Carbopol 940 gel by gradually dispersing 0.2 g of the polymer into 10 mL of aqueous CuNPs (20 mg of CuNPs) under constant stirring. The mixture was stirred for 30 minutes to ensure uniform interaction between the polymer and nanoparticles. Triethanolamine (TEA) was then added dropwise to adjust the pH to 7.0–7.4, neutralizing Carbopol and converting the pre gel into a clear to slightly opaque gel. The formulation was allowed to stand for 2 hours to achieve complete swelling of Carbopol 940, resulting in a viscous, homogeneous gel [53].

2.2.7. Evaluation of the CuNPs

2.2.7.1. Particle size: The average particle size of the synthesized CuNPs was determined via dynamic light scattering (DLS) to assess their uniformity and confirm their nanoscale dimensions.

2.2.7.2. Zeta potential: Zeta potential measurements were performed to evaluate the surface charge and predict the colloidal stability of the nanoparticles.

2.2.7.3. Entrapment efficiency: The percentage of CuNPs successfully incorporated into the gel matrix was quantified to determine the entrapment efficiency, ensuring optimal loading within the polymer network.

2.2.8. Evaluation of the CuNP-Loaded Carbopol Gel

2.2.8.1. Viscosity: The viscosity of the gel was measured via a viscometer to ensure proper consistency and homogeneous distribution of the nanoparticles within the polymer matrix.

2.2.8.2. pH: The pH of the formulation was recorded to confirm its compatibility with physiological conditions and the stability of the gel.

2.2.8.3. Anticancer potential: In vitro cytotoxicity against MCF-7 breast cancer cells was evaluated to assess the therapeutic efficacy of the CuNP-loaded gel.

2.2.8.4. Toxicity Study: Cytotoxicity against normal MCF-10A cells was evaluated to determine the safety profile and selective anticancer activity of the formulation.

2.2.8.5. Drug release: In vitro drug release studies were conducted to determine the release profile of the CuNPs from the Carbopol gel under physiological conditions.

2.2.8.6. Drug release kinetics: The release data were fitted to established kinetic models (e.g., Higuchi, Korsmeyer–Peppas) to elucidate the underlying mechanism of nanoparticle release from the gel matrix.

3. Results and discussion:

3.1. Phytochemical evaluation of extract:

3.1.1. Extraction yield:

The material collected from February–April (late winter to early summer) targets postcool season stress and the onset of flowering, which supports high secondary metabolite biosynthesis; moreover, the sunlight intensity observed during the season is optimal, and low rainfall prevents the leaching of phytoconstituents. Qualitative phytochemical screening of the petroleum ether extract of *Manilkara*

zapota revealed a percent extraction yield of $10 \pm 0.785\%$.

3.1.2. Qualitative Phytochemical Analysis

The analysis revealed the presence of phenols, flavonoids, anthocyanins, steroids, and cardiac glycosides. In contrast, alkaloids, gallic tannins, mucilage, saponosides, resins, quinones, and coumarins were absent, suggesting that the extract is rich in bioactive compounds such as polyphenols and steroids, which may contribute to its potential pharmacological activities.

3.1.3. High-Performance Thin-Layer Chromatography

The extract contained reproducible high-Rf bands at 0.70, 0.76, and 0.88, which were consistent with the sterol/triterpenoid content. Figure 4 demonstrates the image after derivatization under white light with ASR with and without RF tips at 10 μ l of sample petroleum ether extract.

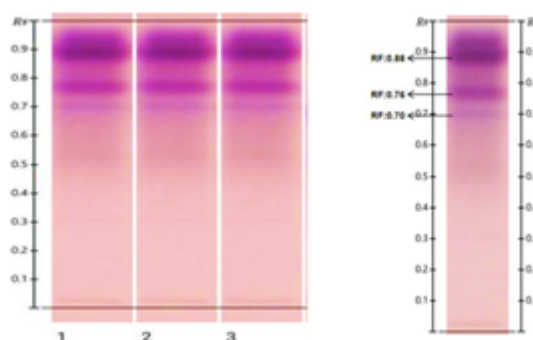


Figure 4. Image after derivatization under white light with ASR without and with RF tips (*Manilkara zapota*). Tracks 1-3: 10 μ l of sample petroleum ether extract.

3.1.4. Gas Chromatography and Mass Spectroscopy

GC-MS analysis of the petroleum ether extract revealed diverse profiles of phytoconstituents dominated by sterols and triterpenoids. According to Table 1 data from the GC-MS study, Cholesta-4,6-dien-3-ol (3β -) was the major component (41.37%), followed by β -sitosterol acetate (10.04%) and 3β -acetoxystigmasta-4,6,22-triene (7.52%), indicating a high sterol content and suggesting potential bioactivity. Other notable constituents included long-chain alkanes, sulfurous acid esters, and minor components such as phytol, 2-methylbutanoate, and borinic acid derivatives, suggesting a complex mixture of lipophilic molecules. The presence of these phytoconstituents implies that the extract may possess anti-inflammatory, antioxidant, or membrane-modulatory properties, aligning with the pharmacological relevance of plant-derived sterols and triterpenoids. Figure 5 gives the GC-MS spectrum of the petroleum ether extract of *Manilkara zapota*, and Figure 6 demonstrates the different structures of constituents observed through GC-MS spectra.

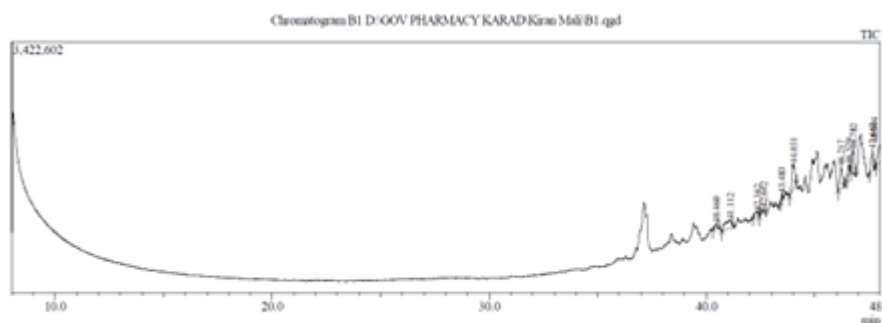


Figure 5 GC-MS spectrum of the petroleum ether extract of *Manilkara zapota*

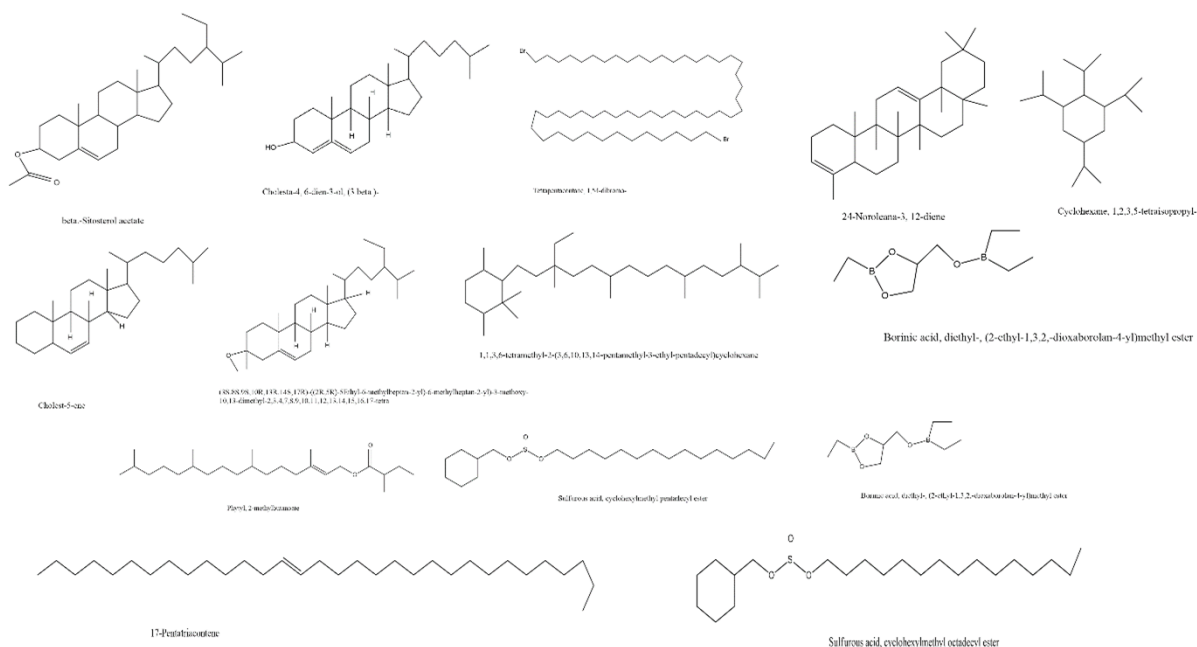


Figure 6. Chemical structures of the different compounds observed via GC-MS analysis

Table 1. GC-MS data for the petroleum extract of *Manilkara zapota*

Peak #	R. Time (min)	I. Time (min)	F. Time (min)	Area	Area %	Name
1	40.460	40.320	40.585	505,242	1.54	Phytyl, 2-methylbutanoate
2	41.112	40.735	41.260	2,570,232	7.82	17-Pentatriacontene
3	42.362	42.170	42.460	587,816	1.79	Sulfurous acid, cyclohexylmethyl pentadecyl ester
4	42.642	42.460	42.705	648,180	1.97	1,1,3,6-tetramethyl-2-(3,6,10,13,14-pentamethyl-3-ethyl-pentadecyl) cyclohexane
5	43.483	43.430	43.550	205,984	0.63	Tetrapentacontane, 1,54-dibromo-
6	44.031	43.845	44.150	3,297,852	10.04	β -Sitosterol acetate
7	46.217	46.075	46.365	2,468,703	7.52	3 β -Acetoxystigmasta-4,6,22-triene
8	46.579	46.475	46.645	763,083	2.32	24-Noroleana-3,12-diene
9	46.782	46.660	46.890	2,214,694	6.74	Sulfurous acid, cyclohexylmethyl octadecyl ester
10	47.662	47.520	47.765	2,002,537	6.10	Cholest-5-ene
11	48.094	47.810	48.165	3,208,554	9.77	(3S,8S,9S,10R,13R,14S,17R)-17-((2R,5R)-5-Ethyl-6-methylheptan-2-yl)-3-methoxy-10,13-dimethyl-2,3,4,7,8,9,10,11,12,13,14,15,16,1
12	48.453	48.395	48.535	326,526	0.99	Borinic acid, diethyl-, (2-ethyl-1,3,2-dioxaborolan-4-yl) methyl ester

13	48.648	48.535	48.795	13,588,875	41.37	Cholesta-4,6-dien-3-ol, (3β)-
14	49.923	49.840	49.965	461,474	1.40	Cyclohexane, 1,2,3,5-tetraisopropyl

3.2. Evaluation of CuNp:

3.2.1. Particle size and zeta potential:

The synthesized copper nanoparticles (CuNPs) had an average size of 282.2 nm, which is within the nanoscale range and favorable for improved cellular uptake and drug delivery (Figure 7). The zeta potential of -6.6 mV (Figure 8) indicates moderate stability in suspension, suggesting that the nanoparticles are reasonably stable and suitable for incorporation into the gel. These characteristics make the CuNPs promising for effective biomedical applications.

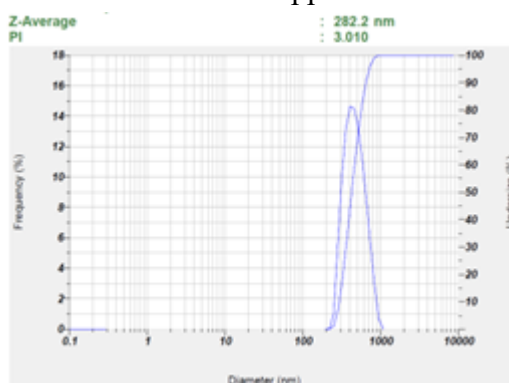


Figure 7. Particle size of copper nanoparticles

Zeta Potential (Mean) : -6.6 mV
 Electrophoretic Mobility Mean : -0.000151 cm²/Vs

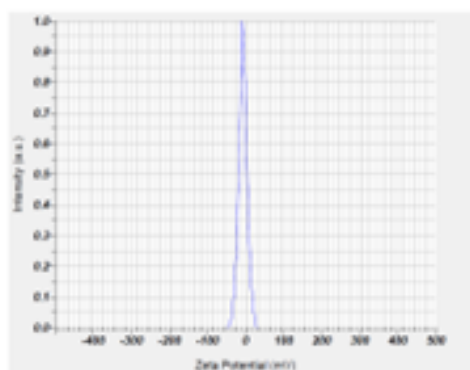


Figure 8. Zeta potential analysis data

3.2.2. Entrapment efficacy:

The percent entrapment efficacy was calculated from the absorbance of the unentrapped extract. The percentage entrapment was approximately 86.83%, which is greater than the accepted range of entrapment for the extract in a copper environment of 80%.

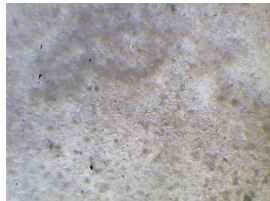
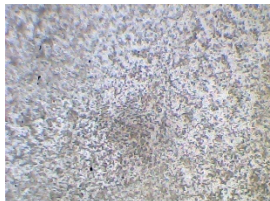
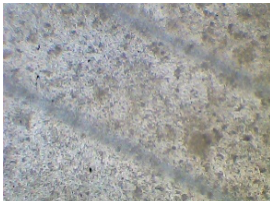
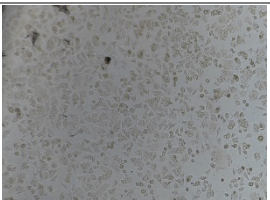
3.3. Physiological evaluation of Carbopol gel:

The prepared gel had a viscosity of 3658.21 cps, indicating a smooth and spreadable consistency that would stay in place without running off, making it comfortable for application. Its pH of 7.36 is close to the natural pH, suggesting that it is likely to be gentle and non-irritating. Overall, these results show that the gel has suitable physical properties for safe and effective topical use.

3.4. Anticancer potential against MCF-7 cells

The anticancer potential of the obtained extract was evaluated against the MCF-7 breast cancer cell line. The standard drug used was 5-fluorouracil, which has an IC₅₀ of 37.16. The results of the petroleum ether extract and gel were compared with those of 5 FU, and the gel showed more potent activity than did the standard. Table No. 2 represents the data on the cell line results against MCF-7.

Table 2 Anticancer cell line study data for MCF-7 cells

Sample	Conc. (µg/mL)	Mean OD	% Inhibition	IC ₅₀ (µg/mL)	
Control (DMSO 0.2%)	—	1.989	—	—	
	10	0.311	84.36	37.16	
	40	0.237	88.08		
100	0.189	90.49			
Petroleum Ether Extract	10	0.803	59.62	36.04	
	40	0.726	63.80		
	100	0.675	66.06		
Gel Formulation	10	0.949	51.89	31.25	
	40	0.872	58.31		
	100	0.751	61.51		

3.5. Toxicity study against MCF 10A

The MCF-10A normal breast epithelial cell line was treated with increasing concentrations (20–100 µg/mL) of petroleum ether extract and its gel formulation. 5-Fluorouracil (5-FU) served as the standard control. Optical density (OD) readings were measured, and percentage inhibition and cell viability were calculated. The MTT assay results revealed that the gel formulation reduced cell viability in a

concentration-dependent manner, indicating its cytotoxic potential. As the concentration increased from 20 to 100 $\mu\text{g/mL}$, the cell viability decreased from 95.82% to 75.52%, with inhibition ranging from 4.18% to 24.48%. In comparison, the standard drug 5-fluorouracil (5-FU) had a slightly stronger effect, reducing viability from 94.84% to 88.12% over the same range. Table 3 represents the data obtained from the cytotoxicity study against MCF-10A. Although the gel was less potent than 5-FU, its gradual and steady reduction in cell viability suggests a sustained release pattern that could help maintain therapeutic levels while reducing side effects. Overall, the results indicate that the gel formulation has promising anticancer activity and could be useful for localized, controlled drug delivery.

Table 3. Cytotoxic effects on MCF-10A cells

Sample	Conc. ($\mu\text{g/mL}$)	OD Mean	% Inhibition	% Viability	IC ₅₀ ($\mu\text{g/mL}$)
Control	–	1.482	–	–	–
5-FU (Standard)	20	1.453	5.15	94.84	NE
	40	1.396	8.87	91.13	
	60	1.387	9.46	90.54	
	80	1.368	10.70	89.30	
	100	1.350	11.87	88.12	
Gel Formulation	20	1.406	4.18	95.82	NE
	40	1.345	8.23	91.77	
	60	1.261	17.99	82.01	
	80	1.210	19.37	80.63	
	100	1.135	24.48	75.52	

In this study, both the petroleum ether extract and the gel showed low cytotoxicity toward MCF-10A cells at concentrations up to 100 $\mu\text{g/mL}$. The percentage yield of viable cells remained above 75% for all the tested concentrations, indicating good biocompatibility with normal breast epithelial cells. The maximum inhibition observed was 21.72% for the extract and 23.41% for the gel at 100 $\mu\text{g/mL}$, suggesting safe concentration ranges for therapeutic applications. IC₅₀ values were not reached within the tested concentration range, which is consistent with minimal cytotoxicity in normal cells.

3.6. Drug release:

The Franz diffusion study revealed that drug release from the gel was influenced by pH. At pH 7.4, the cumulative release was 72.56%, whereas at pH 6.8, it increased to 91.53%. The greater release under mildly acidic conditions may be due to greater polymer relaxation and improved drug solubility, which allows the drug to diffuse more easily through the membrane. Figure 9 gives a graphical representation of cumulative percent drug release vs time. This pH-responsive behavior indicates that the gel can release the drug more effectively in acidic environments such as tumors or inflamed tissues, making it suitable for targeted and controlled drug delivery.

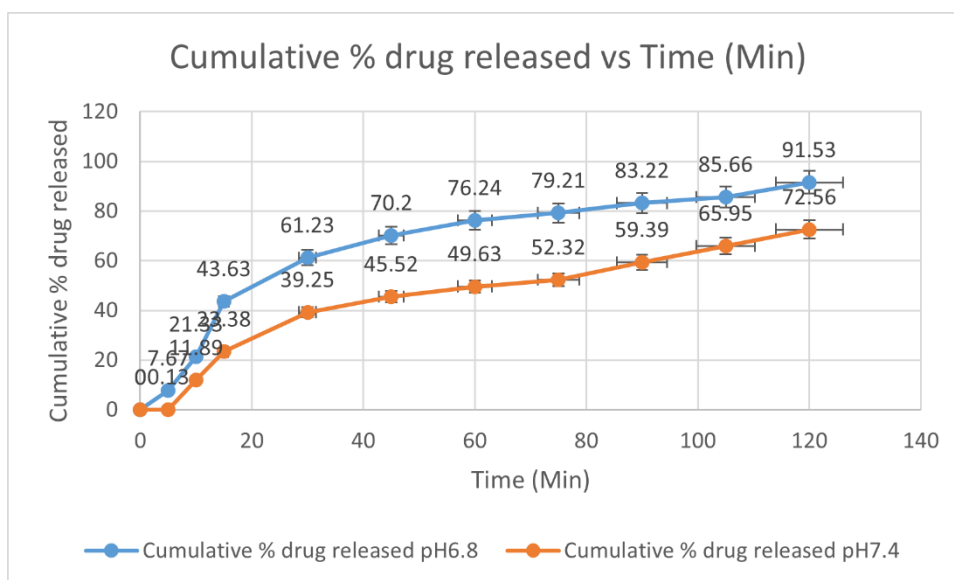


Figure 9. Graphical representation of cumulative percent drug release vs time

3.6.1. Drug release kinetics:

A diffusion kinetic study revealed that the gel released the drug in a sustained and pH-dependent manner, with 91.53% release at pH 6.8 and 72.56% release at pH 7.4. Table 4 represents the R² and the equations obtained from the graphical representation of the kinetic models. The faster release at the mildly acidic pH suggests that the gel becomes more relaxed and allows easier drug diffusion under such conditions, which are similar to those found in tumor or inflamed tissues. The kinetic analysis indicated that the release followed first-order kinetics, meaning that it depended on the remaining drug concentration, whereas the good fit with the Higuchi model confirmed that diffusion played a major role. The Korsmeyer–Peppas model further suggested a non-Fickian (anomalous) release mechanism, where both diffusion and polymer relaxation contributed to the overall process. Together, these findings show that the gel provides a steady, controlled, and pH-responsive release pattern, supporting its potential for targeted and sustained drug delivery.

Table 4 Kinetic release model data at pH 7.4 and 6.8.

Kinetic Model	At 7.4		At 6.8	
	Equation	R ²	Equation	R ²
Kors Pepas	y = 47.256x - 12.503	R ² = 0.9013	y = 31.456x - 10.72	R ² = 0.8581
Zero order	y = 1.2959x + 9.4955	R ² = 0.8824	y = 0.8948x + 3.1662	R ² = 0.9038
higuchi model	y = 11.143x - 6.4435	R ² = 0.9432	y = 7.5243x - 7.133	R ² = 0.9241
First	y = -	R ² =	y = -	R ² =

order	0.0109x + 1.9778	0.9625	0.0054x + 1.9919	0.9408
Hixon Crowel	y = 0.0306x + 0.1142	R ² = 0.9397	y = 0.0172x + 0.0376	R ² = 0.9294

4. Conclusion:

This study highlights the potential of Manilkara zapota petroleum ether extract loaded into copper nanoparticles (CuNPs) as a gel-based anticancer formulation. The extract was rich in bioactive compounds, including sterols, triterpenoids, flavonoids, and phenolics, as confirmed by GC-MS, which identified major constituents such as Cholesta-4,6-dien-3-ol and β -sitosterol acetate, suggesting strong pharmacological potential. The synthesized CuNPs were nanosized (~282.2 nm) with moderate stability (zeta potential of -6.6 mV) and high entrapment efficiency (86.83%), making them suitable for incorporation into a topical gel. The resulting Carbopol gel exhibited ideal physical properties, a good viscosity (3658.21 cps) for easy application and retention, and a skin-friendly pH (7.36), indicating a low risk of irritation. In vitro studies demonstrated that the gel had promising anticancer activity against MCF-7 breast cancer cells, comparable to that of 5-fluorouracil, while showing minimal toxicity toward normal MCF-10A cells, highlighting its safety. Drug release studies revealed pH-responsive behavior, with faster release under mildly acidic conditions (similar to tumor environments), and kinetic analysis confirmed that the release was controlled by both diffusion and polymer relaxation. Overall, the results of this study indicate that the M. zapota-CuNP gel is a safe, effective, and sustained-release system for potential topical anticancer therapy.

5. Future perspectives:

Future studies should focus on evaluating gel formulation in animal models to confirm their anticancer efficacy, safety, and tissue distribution under physiological conditions. Investigating the cellular mechanisms underlying its activity, including uptake and apoptosis pathways, would provide a deeper understanding of its therapeutic potential. Optimization of the gel composition and exploration of combination strategies could further improve release profiles, stability, and targeting efficiency. Additionally, assessing long-term storage stability and scalability is important for clinical translation. In addition to cancer therapy, the bioactive profile of Manilkara zapota suggests that the gel could also be explored for anti-inflammatory, antimicrobial, or wound-healing applications, expanding its range of potential uses.

Funding:

The Project did not receive any funding from any agency.

Consent to Publish declaration:

Not applicable

Consent to Participate declaration:

Not applicable

Ethics declaration:

Not applicable

References:

1. AACR Cancer Disparities Progress Report 2024 Steering Committee, AACR Cancer Progress Report 2024 Steering Committee. Cancer in 2024. Cancer Discovery. 2024 Dec 2;14(12):2324-31.

2. Bilani N, Elimimian EB, Elson L, Liang H, Nahleh Z. Long-term Survivors of breast cancer: a growing population. In *Global Women's Health* 2021 Mar 10. IntechOpen.
3. Traves KP, Cokenakes SE. Breast cancer treatment. *American family physician*. 2021 Aug;104(2):171-8.
4. Sun YS, Zhao Z, Yang ZN, Xu F, Lu HJ, Zhu ZY, Shi W, Jiang J, Yao PP, Zhu HP. Risk factors and prevention of breast cancer. *International journal of biological sciences*. 2017 Nov 1;13(11):1387.
5. Anampa J, Makower D, Sparano JA. Progress in adjuvant chemotherapy for breast cancer: an overview. *BMC Medicine*. 2015 Aug 17;13(1):195.
6. Wali AF, Pillai JR, Talath S, Shivappa P, Sridhar SB, El-Tanani M, Rangraze IR, Mohamed OI, Al Ani NN. Phytochemicals in Breast Cancer Prevention and Treatment: A Comprehensive Review. *Current Issues in Molecular Biology*. 2025 Jan 6;47(1):30.
7. Israel BE, Tilghman SL, Parker-Lemieux K, Payton-Stewart F. Phytochemicals: Current strategies for treating breast cancer. *Oncology letters*. 2018 May;15(5):7471-8.
8. Younas M, Hano C, Giglioli-Guivarc'h N, Abbasi BH. Mechanistic evaluation of phytochemicals in breast cancer remedy: current understanding and future perspectives. *RSC advances*. 2018;8(52):29714-44.
9. Mazurakova A, Koklesova L, Samec M, Kudela E, Kajo K, Skuciova V, Csizmár SH, Mestanova V, Pec M, Adamkov M, Al-Ishaq RK. Anti-breast cancer effects of phytochemicals: primary, secondary, and tertiary care. *EPMA Journal*. 2022 Jun;13(2):315-34.
10. Thakur A, Prasad N, Raina K, Sharma R, Chaudhary A. Role of plant-based anticancer compounds in treatment of breast cancer. *Current Pharmacology Reports*. 2023 Dec;9(6):468-88.
11. Mukherjee AK, Basu S, Sarkar N, Ghosh AC. Advances in cancer therapy with plant based natural products. *Current medicinal chemistry*. 2001 Oct 1;8(12):1467-86.
12. Nounou MI, ElAmrawy F, Ahmed N, Abdelraouf K, Goda S, Syed-Sha-Qhattal H. Breast cancer: conventional diagnosis and treatment modalities and recent patents and technologies. *Breast cancer: basic and clinical research*. 2015 Jan;9: BCBCR-S29420.
13. Chavda VP, Nalla LV, Balar P, Bezbaruah R, Apostolopoulos V, Singla RK, Khadela A, Vora L, Uversky VN. Advanced phytochemical-based nanocarrier systems for the treatment of breast cancer. *Cancers*. 2023 Feb 6;15(4):1023.
14. Shukla S, Shukla AK, Upadhyay AM, Ray N, Fahad FI, Nagappan A, Dutta SD, Mongre RK. Molecular insight and antioxidative therapeutic potentials of plant-derived compounds in breast cancer treatment. *Onco*. 2025 Jun 9;5(2):27.
15. Pandey A, Karmous I. Exploring the Potential of Plant-Based Nanotechnology in Cancer Immunotherapy: Benefits, Limitations, and Future Perspectives. *Biological Trace Element Research*. 2025 Mar;203(3):1746-63.
16. Liyana EP, Jasmine JS. Transformative potential of plant-based nanoparticles in cancer diagnosis and treatment: bridging traditional medicine and modern therapy. *Naunyn-Schmiedeberg's Archives of Pharmacology*. 2025 Apr 16:1-22.
17. Khoobchandani M, Katti KK, Karikachery AR, Thipe VC, Srisrimal D, Dhurvas Mohandoss DK, Darshakumar RD, Joshi CM, Katti KV. New approaches in breast cancer therapy through green

- nanotechnology and nano-ayurvedic medicine—pre-clinical and pilot human clinical investigations. *International journal of nanomedicine*. 2020 Jan 13;181-97.
18. Yang Y, Dong C, Ma X, Wang Y, Li Z, Xu Y, Chen T, Gao C, Ye X, Wu A, Zhang X. Advances in cuproptosis harnessing copper-based nanomaterials for cancer therapy. *Journal of Materials Chemistry B*. 2025;13(9):2978-99.
 19. Zhao F, Zhao Z, Gao H, Zhang Y, Qi J, Yu H, Wang C, Xu J, Yousaf MZ, Che S, Yu J. Cuproptosis: an emerging domain for copper-based nanomaterials mediated cancer therapy. *Med Mat*. 2024 Dec 1;1(2):74-94.
 20. Wang L, Xie Y, Myrzagali S, Pu W, Liu E. Metal ions as effectual tools for cancer with traditional Chinese medicine. *Acupuncture and Herbal Medicine*. 2023 Dec 1;3(4):296-308.
 21. Jagdale S, Samanta R, Narwade M, Haldar N, Jadon R, Gajbhiye V, Gajbhiye KR. Biologically synthesized metallic nanocarriers for efficient therapy of breast cancer. *Expert Review of Anticancer Therapy*. 2025 Aug 3(just-accepted).
 22. Ai L, Yi N, Qiu C, Huang W, Zhang K, Hou Q, Jia L, Li H, Liu L. Revolutionizing breast cancer treatment: Harnessing the related mechanisms and drugs for regulated cell death. *International Journal of Oncology*. 2024 May 1;64(5):1-6.
 23. Biresaw SS, Taneja P. Copper nanoparticles green synthesis and characterization as anticancer potential in breast cancer cells (MCF7) derived from *Prunus nepalensis* phytochemicals. *Materials Today: Proceedings*. 2022 Jan 1;49:3501-9.
 24. Ashokkumar M, Palanisamy K, Ganesh Kumar A, Muthusamy C, Senthil Kumar KJ. Green synthesis of silver and copper nanoparticles and their composites using *Ocimum sanctum* leaf extract displayed enhanced antibacterial, antioxidant and anticancer potentials. *Artificial Cells, Nanomedicine, and Biotechnology*. 2024 Dec 31;52(1):438-48.
 25. Rajagopal G, Nivetha A, Sundar M, Panneerselvam T, Murugesan S, Parasuraman P, Kumar S, Ilango S, Kunjiappan S. Mixed phytochemicals mediated synthesis of copper nanoparticles for anticancer and larvicidal applications. *Heliyon*. 2021 Jun 1;7(6).
 26. Gupta RD, Banerjee S, Basak AK. Bio-metallic copper nanoparticles synthesized from *Cucurbita maxima*: antimicrobial and cytotoxic potential with computational insights into EGFR and VEGFR interactions. *Biochemical and Biophysical Research Communications*. 2025 Jul 12:152318.
 27. Krishna AG, Sahana S, Venkatesan H, Arul V. Green synthesis of copper nanoparticles: a promising solution for drug resistance and cancer therapy challenges. *Journal of the Egyptian National Cancer Institute*. 2024 Dec 28;36(1):44.
 28. Rakshit S, Jana PC, Kamilya T. Green synthesis of copper nanoparticles by using plant extracts and their biomedical applications—an extensive review. *Current Nanomaterials*. 2023 Aug 1;8(2):110-25.
 29. Rakshit S, Jana PC, Kamilya T. Green synthesis of copper nanoparticles by using plant extracts and their biomedical applications—an extensive review. *Current Nanomaterials*. 2023 Aug 1;8(2):110-25.
 30. Baek G, Kim C. Rheological properties of Carbopol containing nanoparticles. *Journal of Rheology*. 2011 Mar 1;55(2):313-30.

31. Ismail SH, Hamdy A, Ismail TA, Mahboub HH, Mahmoud WH, Daoush WM. Synthesis and characterization of antibacterial carbopol/ZnO hybrid nanoparticles gel. *Crystals*. 2021 Sep 7;11(9):1092.
32. Chawla V, Saraf SA. Rheological studies on solid lipid nanoparticle-based carbopol gels of aceclofenac. *Colloids and Surfaces B: Biointerfaces*. 2012 Apr 1; 92:293-8.
33. Meena V, Mathur R, Gull A, Jain N, Madan S. Carbopol thickened nanoemulsions of chemotherapeutics to treat DMBA-induced breast cancer. *International journal of health sciences*.;6(S6):983-99.
34. Thakar B, Agarwal A, Rawal RM. Formulation and evaluation of natural liposomal gel for breast cancer. *Journal of Scientific Research*. 2022 Jan 1;14(1):333-41.
35. Safitri FI, Nawangsari D, Febrina D. Overview: Application of carbopol 940 in gel. In *International Conference on Health and Medical Sciences (AHMS 2020)*, 2021 Jan 27 (pp. 80-84). Atlantis Press.
36. Yusuf AL, Nugraha D, Wahlanto P, Indriastuti M, Ismail R, Himah FA. Formulasi Dan Evaluasi Sediaan Gel Ekstrak Buah Pare (*Momordica Charantia L.*) Dengan Variasi Konsentrasi Carbopol 940. *Pharmacy Genius*. 2022 Oct 20;1(1):50-61.
37. Kaur DA, Raina AP, Singh NI. Formulation and evaluation of carbopol 940-based glibenclamide transdermal gel. *Int J Pharm Pharm Sci*. 2014;6(8):434-0.
38. Ankita K, Asha D, Baquee AA. Formulation and evaluation of a transdermal topical gel of ibuprofen. *J. Drug Deliv. Ther.*. 2020; 10:20-5.
39. Zheng Y, Ouyang WQ, Wei YP, Syed SF, Hao CS, Wang BZ, Shang YH. Effects of Carbopol® 934 proportion on nanoemulsion gel for topical and transdermal drug delivery: A skin permeation study. *International journal of nanomedicine*. 2016 Nov 10:5971-87.
40. Das MK, Ahmed AB. Formulation and ex vivo evaluation of rofecoxib gel for topical application. *Acta Pol. Pharm*. 2007 Sep 1;64(5):461-7.
41. Seshagirirao, K., Harikrishnanaik, L., Venumadhav, K., Nanibabu, B., Jamir, K., Ratnamma, B. K., ... & Babarao, D. K. 2016. Preparation of herbarium specimens for plant identification and voucher number. *R. roxburghii* 6(1-4), 111-119.
42. Babaei Rad S, Mumivand H, Mollaei S, Khadivi A. Effect of drying methods on phenolic compounds and antioxidant activity of *Capparis spinosa L.* fruits. *BMC Plant Biology*. 2025 Jan 31;25(1):133.
43. Chashoo IA, Wani SU, Raja WY, Bhat ZA, Ali M, Alshehri S, Alam P, Ghoneim MM, Asdaq SM, Shakeel F. Physicochemical characterization, phytochemical analysis, and pharmacological evaluation of *Sambucus wightiana*. *Arabian Journal of Chemistry*. 2023 Oct 1;16(10):105170.
44. Nawaz, H., Shad, M. A., Rehman, N., Andaleeb, H., & Ullah, N. 2020. Effect of solvent polarity on extraction yield and antioxidant properties of phytochemicals from bean (*Phaseolus vulgaris*) seeds. *Braz. J. Pharm*, 56, e17129.
45. Bhanwase, A. S., & Alagawadi, K. R. 2016. Antioxidant and immunomodulatory activity of hydroalcoholic extract and its fractions of leaves of *Ficus benghalensis* Linn. *Phcog Res*, 8(1), 50.
46. Adam, O. A. O., Abadi, R. S. M., & Ayoub, S. M. H. 2019. The effect of extraction method and solvents on the yield and antioxidant activity of certain Sudanese medicinal plant extracts. *J Phytopharmacol* 8(5), 248-252.

47. Dhanani, T., Shah, S., Gajbhiye, N. A., & Kumar, S. 2017. Effect of extraction methods on yield, phytochemical constituents, and antioxidant activity of *Withania somnifera*. Arab. J. Chem., 10, S1193-S1199.
48. Joseph, N., Sorel, N. E. M., Kasali, F. M., & Emmanuel, M. M., 2015. Phytochemical screening and antibacterial properties from the extract of *Alchornea cordifolia* (Schumach. &Thonn.) Müll. Arg. J. Pharmacogn. Phytochem., 4(3), 176-180.
49. Limpabandhu, T., Suwatronnakorn, M., Widoyanti, A. A. E., Issaravanich, S., Zongrum, O., & Prasansuklab, A. 2024. Pharmacognostic standardization and phytochemical evaluation of *Ficus rumphii* Blume leaves in Thailand. Phytomed. Plus, 4(4), 100661.
50. Shaikh, J. R., & Patil, M. 2020. Qualitative tests for preliminary phytochemical screening: An overview. Int. J. Chem. Stud 8(2), 603-608.
51. Pudumo, J., Chaudhary, S. K., Chen, W., Viljoen, A., Vermaak, I., & Veale, C. G. L. 2018. HPTLC fingerprinting of *Croton gratissimus* leaf extract with Preparative HPLC-MS-isolated marker compounds. S Afr J Bot 114, 32-36.
52. Biresaw SS, Taneja P. Copper nanoparticles green synthesis and characterization as anticancer potential in breast cancer cells (MCF7) derived from *Prunus nepalensis* phytochemicals. Materials Today: Proceedings. 2022 Jan 1;49:3501-9.
53. Tilawat M, Bonde S. Curcumin and quercetin loaded nanocochleates gel formulation for localized application in breast cancer therapy. Heliyon. 2023 Dec 1;9(12).